Peer-reviewed version available at *Pharmaceutics* **2019**, *11*, 284; doi:10.3390/pharmaceutics11060284

Article

Ucuùba (*Virola surinamensis*) Fat-based Nanostructured Lipid Carriers for Nail Drug Delivery of Ketoconazole: Development and Optimization Using Box- Behnken Design

Rayanne R. Pereira[1,2], Matteo Testi[2], Francesca Rossi[3], Jose O.C. Silva Junior[1], Roseane M. Ribeiro-Costa[1], Ruggero Bettini[2,4], Patrizia Santi[2,4], Cristina Padula[2], Fabio Sonvico[2,4,*]

[1] Pharmaceutical Sciences Faculty, Federal University of Para, Belem (Brazil); rayannerocha@yahoo.com (R.R.P.); carrera@ufpa.br (J.O.C.S.J.); rmrc@ufpa.br (R.M.R.C.).
[2] Food and Drug Department, University of Parma, Parma (Italy); matteo.testi1@studenti.unipr.it (M.T.); patrizia.santi@unipr.it (P.S.); cristina.padula@unipr.it (C.P.)
[3] Institute of Materials for Electronics and Magnetism (IMEM), CNR - Italian National Research Council, Parco Area delle Scienze 37/A, Parma, Italy; francesca.rossi@imem.cnr.it (F.R.)
[4] Biopharmanet-TEC, University of Parma, Parma (Italy) ruggero.bettini@unipr.it (R.B.); fabio.sonvico@unipr.it (F.S.)

* Correspondence: fabio.sonvico@unipr.it; Tel.: +39-0521-906282

Abstract: Ucuùba fat is fat obtained from a plant found in South America, mainly in Amazonian Brazil. Due to its biocompatibility and bioactivity, the Ucuùba fat was used for production of ketoconazole-loaded nanostructured lipid carriers (NLC) in view of an application for the treatment of onychomycosis and other persistent fungal infections. The development and optimization of the Ucuùba fat based NLC were performed using a Box-Behnken design of experiment. The independent variables were surfactant concentration (% w/v), liquid lipids concentration (% w/v), solid lipids concentration (% w/v), while the outputs of interest were particle size, polydispersity index (PDI) and drug encapsulation efficiency (EE). The Ucuùba fat based NLC were produced and the process optimized determining a predictive mathematical model. Applying the model, two formulations with the pre-required particle size, *i.e.* 30 and 85 nm, were produced for further evaluation. The optimized formulations were characterized and showed a particle size in agreement to the predicted value, *i.e.* 33.6 nm and 74.6 nm, respectively. The optimized formulations were also characterized using multiple techniques in order to investigate the solid state of drug and excipients (DSC and XRD), particle morphology (TEM) and interactions between the formulation components (FTIR). Furthermore, particle size and surface charge of the formulations was studied during a one-month stability study and did not evidence any significative modification during storage.

Keywords: Amazonian fat; Ucuùba fat; Box Behnken Design; Solid lipid nanoparticles; Antifungal therapy; Onychomycosis.

1. Introduction

Onychomycosis is the most common nail disease of nail plate and nail bed [1–3]. Several antifungal agents are used in the treatment of onychomycosis, among them ketoconazole, an imidazole derivative that acts by blocking the synthesis of ergosterol. Oral treatment of onychomycosis with ketoconazole provides a cure rate of 50 to 70% in fingernail and 15 to 30% in toenail infections [4,5]. However oral treatment has several disadvantages, such as long duration, drug interactions, systemic side effects, and high rates of recurrence. In this regard, topical treatment

Peer-reviewed version available at Pharmaceutics 2019, 11, 284; doi:10.3390/pharmaceutics11060284

appears advantageous and in fact several topical preparations are on the market containing 2% ketoconazole in the form of gel, cream or lotions. However, the topical treatment available has the disadvantage of low permeation of the drug through the nail [4,6,7].

Nanostructured lipid carriers (NLC) are colloidal dispersions in which the dispersed phase is composed of a mixture of both solid and liquid lipids stabilized by an emulsifier [8,9] . Lipid nanoparticles has been extensively used for topical application, since their lipid matrix can interact with the lipids of the *stratum corneum*, promoting drug delivery to the skin. Moreover, the occlusive film formed by lipid nanoparticles on the skin surface significantly increases tissue hydration and drug skin permeation [10–12]. It has been shown that lipid nanocarriers are also be capable of increasing nail plate hydration enhancing drug penetration [13] .

The solid lipid selected for production NLC has a pivotal role, because it affects a number of physicochemical and biopharmaceutical properties of the particles (surface charge, melting point, drug loading and release properties among others) [14,15]. Plant derived fats are a viable option, since they are made of essential fatty acids important for maintaining the homeostatic balance of the skin and its annexes [16,17]. Ucuùba butter (*Virola surinamensis*) is extracted from the seeds of Ucuùba, a tree found mainly in the Amazon river basin, but present in an area that encompasses all of Central America and part of South America. Traditional uses of this fat span from the production of candles to medical soaps, but Ucuùba butter can be found also as a component of moisturizing creams and shampoos in the Brazilian cosmetic market [16,18] . The main fatty acids present in Ucuùba fat are myristic and lauric acid, while oleic, palmitoleic, linoleic acids are present at lower concentrations [19]. In addition, the presence in the leaves, root, bark and seeds of *V. surinamensis* of phenylpropanoids, propiophenones, lignans, neolignans, polyketides and flavonoids with anti-oxidant, anti-inflammatory and anti-mycotic action has been reported in other studies and elicited interest in the pharmaceutical properties of this fat [20–22].

In several studies related to the optimization of NLC production it is observed that the choice of the relative concentration of surfactant and lipids strongly affect the stability of the formulation [23] . Furthermore, also the physical-chemical characteristics of NLC, such as size, entrapment efficiency (EE), physical stability, drug release, morphology, are strongly influenced by the choice and amount of lipids and surfactant [23–25]. Thus, an optimization of NLC production with the aid of design of experiment could be carried out with the objective of modulating the amount of liquid and solid lipids and surfactant to obtain the most desirable properties in terms particle size, entrapment efficiency and stability. Response surface method (RSM) is one of the prevalent approaches in design of experiments, which involves the use of different type experimental designs to generate polynomial mathematical relationships mapping of the response over the experimental domain with the aim to predict the outcome of a process or select the optimal process parameters [26]. Box-Behnken design (BBD) is one of RSM approaches, which is an independent, rotatable or nearly rotatable, quadratic design having the process variable combinations at the midpoints of the edges of the process space and its centre. A significative advantage of the Box-Behnken design is that it is more cost effective if compared with the other techniques such as Central Composite Design, 3-levels factorial design and D-optimal design, as it requires fewer experimental runs and less time for process optimisation [26,27].

We hypothesized that Ucuùba fat, on account of its physicochemical and biological properties, could be a suitable lipid excipient for the production of NLC loaded with ketoconazole. Thus, the objective of this work was to obtain and optimize ketoconazole-loaded NCL production by high pressure optimization using Ucuùba fat in oily phase. The Design of Experiment was then applied to select the optimal conditions for the production of Ucuùba fat-based NLC in terms of encapsulation efficiency (EE), particle size and polydispersity index (PDI) in view of their use as a nail drug delivery system.

Peer-reviewed version available at Pharmaceutics 2019, 11, 284; doi:10.3390/pharmaceutics11060284

2. Materials and Methods

2.1. Materials

Virgin Ucuùba fat (*V. surinamensis)* was provided by Amazon Oil Industry (Ananindeua, Brazil). D-α-Tocopheryl polyethylene glycol 1000 succinate (TPGS 1000) was supplied by ISOCHEM (Gennevilliers, France). Propylene glycol monocaprylate (type II) (Capryol™ 90) acquired Gattefossé (Saint Priest, France). Ketoconazole was purchased Galena (São Paulo, Brazil). All other reagents were of analytical purity grade. Ultrapure (0.055 μS/ cm, TOC 1 ppb) was obtained with a Purelab Pulse + Flex Ultrapure water system (Elga Veolia, Milan, Italy).

2.2. Ucuùba fat-based NLC preparation

Ucuùba fat NLC were prepared using an emulsification, homogenization and solidification technique. The lipid phase was prepared by melting Ucuùba fat at 10°C above the lipid melting point and by mixing the liquid lipid with TPGS 1000, Capryol™ 90 and ketoconazole (0.5% w/v). Then, the aqueous phase, preheated at 70°C, was added gradually into the lipid phase under continuous magnetic stirring. Subsequently, a pre-emulsion was prepared using (Ultra-Turrax® TP18/10, IKA Werke GmbH&Co., Staufen, Germany) operated at 10,000 rpm for 1 minute. Finally, the pre-emulsion was processed using laboratory High Pressure Homogenizer (HPH) (Panda Plus 2000, GEA Niro Soavi S.p.A., Parma, Italy) at 70°C for 10 successive cycles at the pressure of 500 bar. Nanoparticles were then left to cool to ambient temperature.

2.3. Experimental design

A three-level three-factor (3^3) Box-Behnken design (BBD) was applied for NLC production optimization process using the statistical package Desing-Expert® Software (version 11, Stat-Ease Inc., Minneapolis, MN, USA). To this purpose, we selected three input factors, or critical process parameters (CPPs), namely: the concentration of the surfactant (TPGS), the concentration of liquid lipid (Capryol 90) and the concentration of the solid lipid (Ucuùba fat). These input factors were set at three levels, i.e. low, middle and high values, indicated conventionally by -1, 0 and +1, respectively. The design, including five repetitions of the central point, included a total of 17 experiments. The measured responses, or critical quality attributes (CQAs), were particle size (Y_1), polydispersity index (PDI) (Y_2) and encapsulation efficiency (EE) (Y_3) (see **Table 1**).

For each CQA, the influence of the input factors and their interactions on the responses can be described for the non-linear quadratic model generated by the design was:

$$Y = A_0 + A_1X_1 + A_2X_2 + A_3X_3 + A_4X_1X_2 + A_5X_2X_3 + A_6X_1X_3 + A_7X_1^2 + A_8X_2^2 + A_9X_3^2, \quad (1)$$

in which Y is the predicted response, A_0 is intercept, A_1-A_9 are the regression coefficients values. X_1, X_2 and X_3 are codes for independent variables, concentration of the surfactant, concentration of liquid lipid and the concentration of lipid solid, respectively. The terms (X_1X_2, X_2X_3 and X_1X_3) and (X_i^2, where i= 1,2 and 3) represent the factors interactions and quadratic terms respectively.

Peer-reviewed version available at Pharmaceutics 2019, 11, 284; doi:10.3390/pharmaceutics11060284

Table 1 Input factors and their levels for Box-Behnken design

Input factors	Levels		
	-1	0	+1
Surfactant Concentration (% w/v, X_1)	3	4.5	6
Liquid Lipid Concentration (% w/v, X_2)	2	2.5	3
Solid Lipid Concentration (% w/v, X_3)	7	7.5	8

2.4. Ucuùba fat-based NLC Characterization

2.4.1. Particle Size Distribution

Ucuùba fat-based NLC were characterized by dynamic light scattering using a Zetasizer Nano ZS (Malvern Pananalytical, Malvern, UK) applying Non-Invasive Back-Scatter (scattering angle 173°) at the temperature of 25°C. NLC were diluted (1:100) with ultrapure water prior to measurements. Optimized NLC were at different days (0, 1, 7, 15 and 30 days). Average particle size (Z-average) and polydispersity index (PDI) obtained through the cumulants analysis of scattering data by the instrument software were measured in triplicate and results were expressed as mean and standard deviation.

2.4.2 Zeta Potential

The zeta potential, representative of particle surface electrostatic charge, was determined by electrophoretic mobility (Zetasizer Nano ZS, Malvern, Pananalytical, Malvern, UK). The samples were diluted in 10 mM NaCl (1:500). Helmoltz-Smoluchowski equation was employed for calculation of zeta potential by the instrument software.

2.4.2 Encapsulation Efficiency (EE)

The content of ketoconazole in nanoparticles was determined by the high-performance liquid chromatography (HPLC). The analysis was carried out on a Shimadzu chromatography system consisting of an autosampler (Model 542, ESA Biosciences, Chelmsford, MA, USA), a pump (LC-10AS, Shimadzu, Kyoto, Japan) and an UV-VIS detector (SPD-10 A, Shimadzu, Kyoto, Japan). A reverse phase C18 column (YMC-Pack ODS-AQ, 250 x 4.6 mm, particle size 5µm, pore size 120 Å, YMC Co. Ltd., Kyoto, Japan) was employed for chromatographic separation in combination with a mobile phase consisting of a 75:25 (v/v) mixture of 0.5% w/v triethanolamine in methanol and 0.2% w/v ammonium acetate (pH 5). HPLC analyses were carried out at a flow rate 0.8 mL/min, detection wavelength 240 nm at 25°C. Sample injection volume was 20µL and sample elution time 10 minutes.

Linearity of response in calibration curves for ketoconazole was verified in the range of 1-3–µg/mL (r^2=0.999). Limit of detection and limit of quantification were 0.18 and 0.56 µg/mL, respectively.

The encapsulation efficiency (EE) of nanoparticles was determined by an indirect method, that is the amount of ketoconazole precipitated or present in agglomerates was quantified and subtracted from the total amount of drug present in the whole NLC dispersion. Firstly, a precise volume of Ucuùba fat-based NLC preparation was dispersed in the mobile phase in order to extract the drug and quantitate the total drug present in the formulation by HPLC analysis. The second step consisted in separating and determine the precipitated drug from the encapsulated drug. In order to separate the drug present as crystals or particle agglomerates, the formulation was centrifuged at 9,500×g at 25°C for 15 min (Model D3024, Scilogex, USA). The supernatant was discarded without troubling the sedimented drug present as agglomerate or precipitated drug. The pellet was then solubilized in

Peer-reviewed version available at Pharmaceutics 2019, 11, 284; doi:10.3390/pharmaceutics11060284

mobile phase and analysed by HPLC. The EE were calculated using Equation (1), also considering the poor aqueous solubility of ketoconazole [28].

$$EE\ (\%) = \frac{(Total\ drug - Precipitated\ drug)}{Total\ drug} \times 100 \quad (1)$$

2.4.3. Morphology

Transmission Electron Microscopy (TEM) analysis of the NCL produced was carried out using a JEM 2200-FS microscope (JEOL Ltd., Tokyo, Japan) operated at 80 kV. For sample preparation, a drop of the suspension was deposed on formvar/carbon coated copper grids (300 mesh, Electron Microscopy Sciences, Holfield, PA, USA), after 60 seconds the excess was gently dried with filter paper and grid was stained using a drop of a 2% w/v solution of uranyl acetate (Sigma Aldrich, St. Louis, MO, USA) for 120 seconds. The staining solution was gently eliminated with filter paper and the grid rapidly dipped in particle free ultrapure water to further eliminate loosely bound material and excess staining residuals. The images were processed with Digital Micrograph software (Gatan Inc., Pleasanton, Ca, USA).

2.4.4. Differential scanning calorimetry (DSC)

Differential scanning calorimetry was performed using a Mettler-Toledo DSC823e equipment (Schwerzenbach, Switzerland). All the samples NLC, ketoconazole and excipients (mixtures Capryol 90 and Ucuùba fat 3:1, 1:1 and 1:2) were prepared introducing 1- 5 mg of sample in aluminium pans sealed and double pierced. Thermal scans were recorded from 15 to 100°C for the lipid mixtures and from 15 to 200°C for the NLC samples at a heating rate of 10°C/ min under dry nitrogen purge (80 mL/ min).

The samples of the NLC were air dried for 4h at room temperature for DSC analysis. Lipid mixtures were magnetically stirred at 200 rpm for 1h at 70°C for complete homogenization between lipids. The degree of crystallinity of mixtures of virgin Ucuùba fat and Capryol 90 was determined by calculating the crystallinity index (CI) from the heat of fusion using Equation (2) [29]:

$$CI(\%) = \left(\frac{\Delta H_{mix}}{\Delta H_{PL}}\right) \cdot f_{mix} \cdot 100 \quad (2)$$

where ΔH_{mix} is the enthalpy of fusion of the lipid mixture, ΔH_{PL} is the fusion enthalpy of the pure lipid, and f_{mix} is the weight fraction of the solid lipid in the mixture.

2.4.5 X- ray diffraction (XRD)

X-ray diffraction (XRD) of the NLC formulation and the Ucuùba fat was performed using a MiniFlex X-Ray Diffractometer (Rigaku, Japan) using Cu K_α radiation (λ= 1.5418 Å) generated with 30 kV. About 200 mg of air dried NLC formulation and Ucuùba fat were loaded on the sample holder until it was completely full and then pressed with a glass slide in order to obtain a flat and homogeneous surface. The samples were analyzed from a starting angle θ of 2° to an end angle of 35° with a scanning rate of 1.5 ° min^{-1} (step size 0.5°).

2.4.6 Infrared Spectroscopy

The absorption spectra of the excipients, *i.e.* Capryol 90, Ucuùba fat and ketoconazole, and NLC formulations, were analyzed using a Shimadzu spectrophotometer (IR Prestige 21, Kyoto, Japan) in the range 4,000-1,000 cm^{-1}. The samples were dripped in tablets of potassium bromide and spectra recorded using 32 scans and 2 cm^{-1} resolution at room temperature [30].

Peer-reviewed version available at Pharmaceutics 2019, 11, 284; doi:10.3390/pharmaceutics11060284

3. Results

3.1. Design of Experiment

In this study, a Box-Behnken design was applied in order to evaluate the interactions and the main quadratic effects of selected at different levels on three critical quality attributes, *i.e.* NLC particle size, polydispersity index and encapsulation efficiency. **Table 2** the Box- Behnken design results are summarized.

The mean particle size (response Y_1) ranged from 23.94 nm (Experiment 16) to 90.13 nm (Experiment 08) depending on variables level selected during production in **Table 2**. PDI values (response Y_2) ranged from 0.248 (Experiment 7) to 0.558 (Experiment 2) indication that there were formulations with distributions from mostly unimodal to multimodal size distributions. The encapsulation efficiency (EE, response Y_3) varied from 93.91% (Experiment 1) to 99.66% (Experiment 5) (see **Table 2**). The ratio between maximum and minimum values for responses Y_1, Y_2 and Y_3 was found to be 3.76, 2.25 and 1.06, indicating no requirement of power transformation of values.

Table 2. Results of the experiments of the Box-Behnken design

Experiment #	Surfactant (% w/v)	Liquid Lipid (% w/v)	Solid Lipid (% w/v)	Size (nm)	PDI[1]	Ketoconazole EE[2] (%)
1	4.5	2	8	65.9	0.506	93.91
2	3	2.5	8	79.4	0.248	98.71
3	6	2.5	7	26.6	0.432	96.05
4	4.5	3	8	68.0	0.413	97.16
5	4.5	3	7	45.1	0.492	99.66
6	4.5	2.5	7.5	45.4	0.36	97.75
7	3	2	7.5	82.1	0.291	94.67
8	3	3	7.5	90.1	0.311	97.26
9	4.5	2.5	7.5	47.6	0.399	97.67
10	6	2.5	8	39.8	0.533	97.99
11	6	2	7.5	66.8	0.558	96.38
12	4.5	2.5	7.5	43.3	0.449	98.56
13	4.5	2	7	54.0	0.481	97.95
14	4.5	2.5	7.5	48.1	0.329	99.50
15	3	2.5	7	69.8	0.263	96.55
16	6	3	7.5	23.9	0.288	98.29
17	4.5	2.5	7.5	63.0	0.461	96.57

[1] Polydispersity Index

[2] Encapsulation Efficiency

It was observed that the best fitted model was quadratic for all considered responses. The results of the analysis of variance (ANOVA) performed to investigate the models for the three responses (particle size, Y_1; PDI, Y_2; encapsulation efficiency, Y_3) are shown in **Table 3**. The significance of the regression coefficients for the input factors was evaluated by the correspondent p-value (<0.05) calculated by ANOVA (see Table 3). The p-values were used as tool to check the significance of each coefficient for understand the pattern of the mutual interactions between the selected process parameters. The smaller the magnitude of the p-value, the more significant is the corresponding coefficient. A p-value below 0.05 was considered an indication of a significant contribution of the factor (see **Table 3**). The fit of the model was evaluated by coefficient of determination (R^2).

Table 3. ANOVA results obtained for the regression model obtained from the experimental design for the prediction particle size, PDI and EE.

	Particle Size (Y_1)			PDI (Y_2)			EE (Y_3)		
Factors	**Coefficient Estimate**	**F-value**	**p-value**	**Coefficient Estimate**	**F-value**	**p-value**	**Coeficient Estimate**	**F-value**	**p-value**
Intercept	49.49	11.56	0.0020*	0.3996	4.26	0.0346*	98.1	0.64	0.7392
X_1	-20.54	66.07	0.0001*	0.0873	17.58	0.0041*	0.1900	0.10	0.7649
X_2	-5.21	4.24	0.0784	-0.0415	3.98	0.0864	1.18	3.74	0.0942
X_3	7.19	8.10	0.02*	0,0040	0.04	0.8530	-0.3050	0.25	0.6330
X_1X_2	-12.73	12.69	0.0092*	-0.0725	6.07	0.0433*	-0.1700	0.04	0.8497
X_1X_3	0.8825	0.06	0.8120	0,0290	0.97	0.3573	-0.0550	0.00	0.9510
X_2X_3	2.76	0.59	0.4660	-0.0260	0.78	0.4063	0,3850	0.20	0.6695
X_1^2	5.96	2.93	0.1307	-0.0708	6.09	0.0430*	-0.6025	0.51	0.4976
X_2^2	10.29	8.73	0.0212*	0.0332	1.34	0.2851	-0.7575	0.81	0.3984
X_3^2	-1.56	0.20	0.6682	0,0332	1.96	0.2038	-0.0825	0.01	0.9247
Model									
R^2		0.9369			0.8456			0.4513	
F- value		11.48			4.33			0.6347	

* Significant effect of the factor on individual responses.

Abbreviations: ANOVA, analysis of variance; PDI, polydispersity index; EE, encapsulations efficiency; X_1 surfactant concentration; X_2 liquid lipid concentration; X_3 solid lipid concentration; F-value, ratio of the mean regression sum of squares divided by the mean error sum of squares; R^2, coefficient of determination.

Peer-reviewed version available at Pharmaceutics 2019, 11, 284; doi:10.3390/pharmaceutics11060284

3.1.1 Particle size

In the case of particle size, the value of coefficient of determination ($R^2 = 0.9369$) of the quadratic model indicated that only 6.31% of the total variations was not explained by the model (see **Table 3**). The quadratic model correlating input factors to particle size resulted in the polynomial Equation (3) and allowed to design three response surface graphs (Figure 1) for the optimization lipid nanoparticle size.

$$Y_1 = 49.49 - 20.54X_1 - 5.21X_2 + 7.19X_3 - 12.73X_1X_2 + 0.88X_1X_3 + 2.76X_2X_3 + 5.96X_1^2 + 10.29X_2^2 - 1.56X_3^2 \quad (3)$$

The concentration of surfactant (X_1), liquid lipid (X_2^2), solid lipid (X_3) and interaction between surfactant and liquid lipid (X_1X_2) and were the factors significantly affecting ($p < 0.05$) the particle size (Y_1) according to ANOVA (see **Table 3**). A positive coefficient value before a factor in the regression equation indicates that the response increases along with the factor and *vice versa*. The coefficient values show that particle size is strongly dependent from concentrations of TPGS. In fact, as shown in Figure **2a**, when maintaining the Ucuùba fat (solid lipid) concentration constant, lipid nanoparticles particle size decreased when the concentrations of Capryol 90 (liquid lipid) and TPGS (surfactant) increased (Figure **1a**).

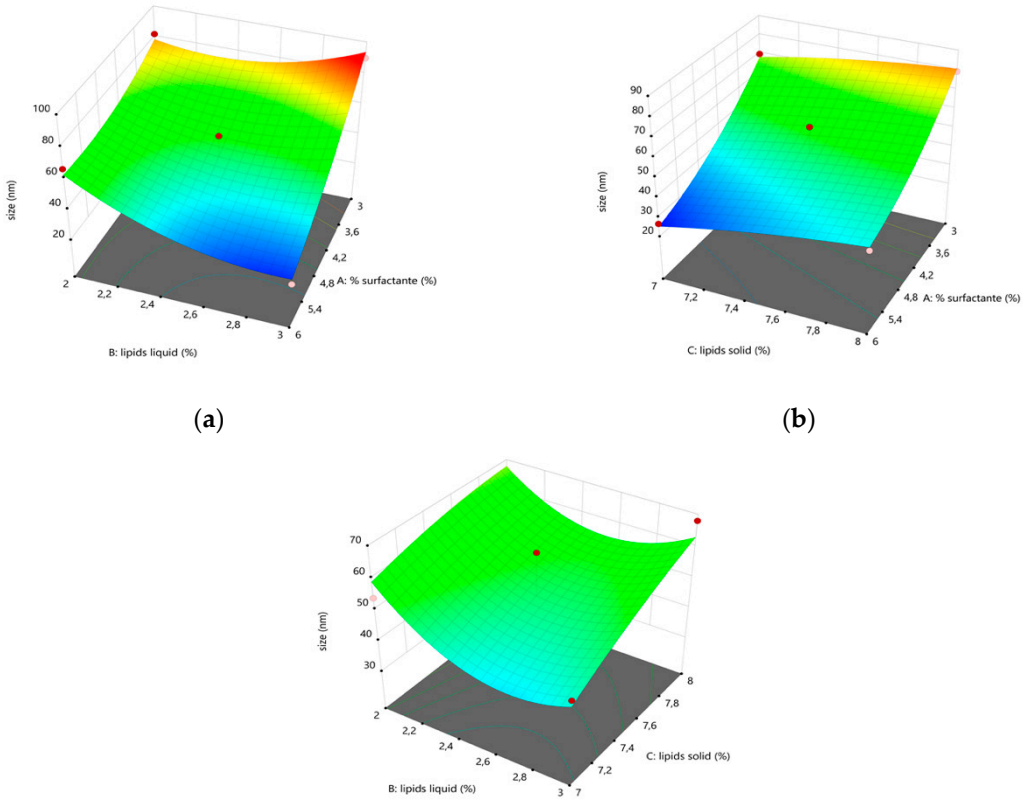

(**a**) (**b**)

(**c**)

Figure 1. Three-dimensional response surface plots showing the effect of **(a)** the concentration of liquid lipid and surfactant, **(b)** the concentration of surfactant and solid lipid and **(c)** the concentration of liquid lipid and solid lipid on NLC particle size, respectively.

Similarly, blocking the concentration of Capryol 90 and varying the concentrations of TPGS and Ucuùba fat, it was observed a decrease of lipid nanoparticles particle size with the increase of the

Peer-reviewed version available at Pharmaceutics 2019, 11, 284; doi:10.3390/pharmaceutics11060284

surfactant concentration and the decrease of the Amazonian fat concentration (Figure **1b**). On the other hand, when the concentration of the surfactant was maintained constant and the concentration of lipids was varied (Figure **1c**), no significant variations in terms of particle size were observed.

3.1.2. Polydispersity Index (PDI)

For PDI, the value of coefficient of determination of the quadratic was R^2=0.8477 indicating that 15.23% of the total variations was not explained by the model, an higher when compared with the 6.31% the particle size related model (see all the values in **Table 3**).

The effect of the selected factors on PDI was described by the quadratic Equation (4).

$$Y_2 = 0.400 + 0.087X_1 - 0.041X_2 + 0.004X_3 - 0.073X_1X_2 + 0.029X_1X_3 - 0.026X_2X_3 - 0.071X_1^2 + 0.033X_2^2 - 0.040X_3^2 \quad (4)$$

According to ANOVA the significant factor was the concentration of the surfactant and the combination of surfactant and liquid lipid concentrations. Figure **2** shows the response surface plots correlating the PDI to the factors investigated.

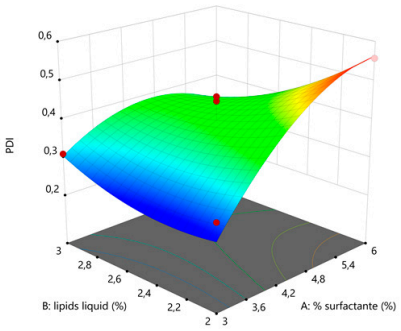

(a)

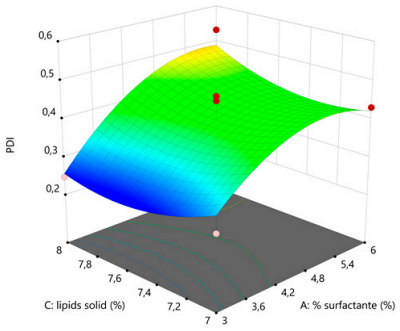

(b)

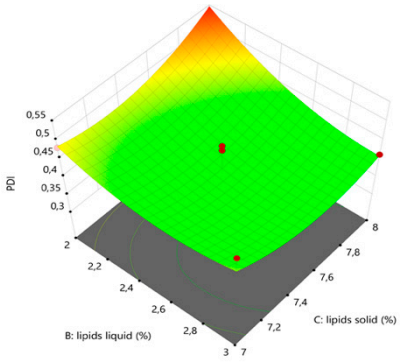

(c)

Figure 2. Three-dimensional response surface plots showing the effect of **(a)** the concentration of liquid lipid and surfactant, **(b)** the concentration of surfactant and solid lipid and **(c)** the concentration of liquid lipid and solid lipid on NLC polydispersity index (PDI), respectively.

Peer-reviewed version available at Pharmaceutics 2019, 11, 284; doi:10.3390/pharmaceutics11060284

Analysing the response surfaces for PDI, again it appears that this nanoparticle attribute was mainly influenced by surfactant concentration (Figure **2a** and **2b**). However, differently from particle size, PDI steeply increased when the TPGS concentration was increased. The Ucuùba fat and Capryol 90 concentrations (Figure **2c**) appeared to be less relevant for PDI values compared to their effect combined with surfactant variations, even if a tendency to an increase of the PDI when both the solid lipid to liquid lipid concentrations increase is evident. In any case, the response surface plot representing Ucuùba fat and Capryol 90 interaction, keeping constant TPGS concentration, resulted overall in a not significant PDI variation.

3.1.3. Ketoconazole Encapsulation Efficiency

The model correlating ketoconazole encapsulation efficiency to the selected factors was found to be not significant (R^2=0.4513, p-value 0.7392). Then, within the present design space it was not possible to achieve a significant different in terms of entrapment efficiency. It was possible to evidence that ketoconazole at the selected concentration of 0.5% w/v could be efficiently loaded into nanostructured lipid carriers obtained using TPGS surfactant, Capryol 90 as liquid lipid, and Ucuùba fat as solid lipid within the range of concentration tested (Figure **3**).

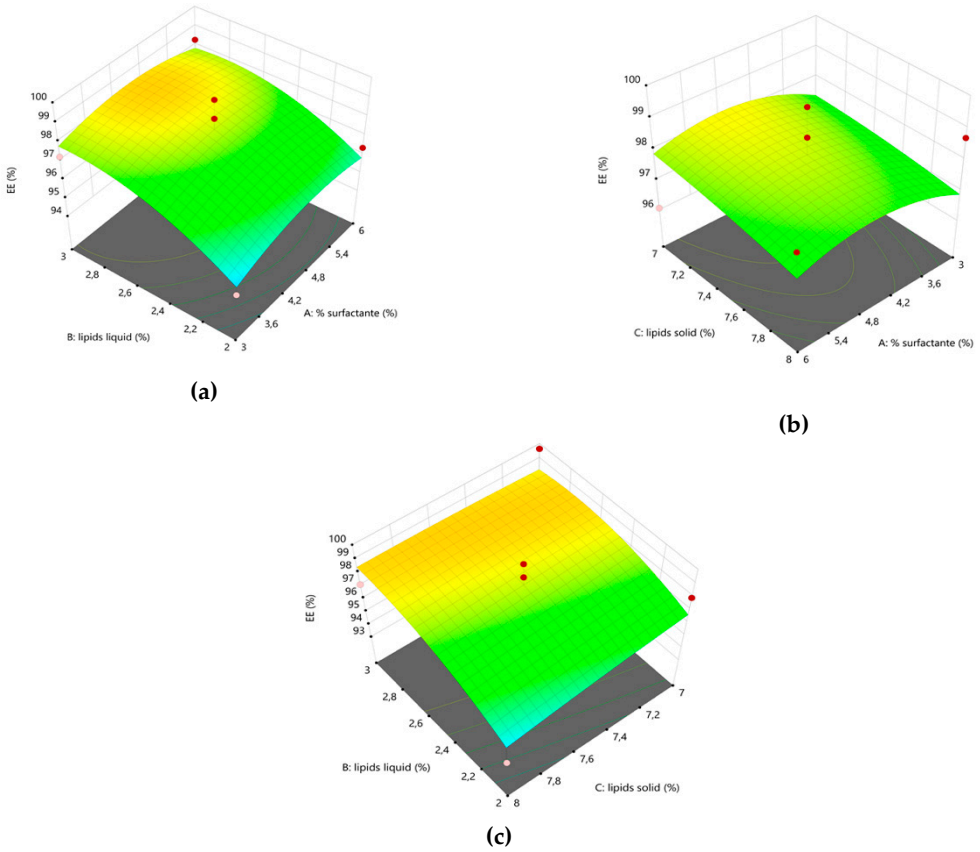

Figure 3. Three-dimensional response surface plots showing the effect of the concentration of liquid lipid and surfactant **(a)**, the concentration of surfactant and solid lipid **(b)** and the concentration of liquid lipid and solid lipid **(c)** on NLC ketoconazole encapsulation efficiency (EE), respectively.

3.1.4. Formulation optimization and model validation

A desirability function was applied to the models obtained to identify the process parameters required to prepare optimized formulations. The optimal formulation was based on the criteria of maximum entrapment efficiency, minimum PDI and specific particle size. The actual values of the dependent variables at the optimal combination of factors suggested by the software were assessed

Peer-reviewed version available at Pharmaceutics 2019, 11, 284; doi:10.3390/pharmaceutics11060284

to confirm the validity of the calculated optimal factors by expected responses. In particular two optimized formulations were prepared using the model, one with smaller (30 nm, F 30) and a second with larger (85 nm, F 85) required particle size, respectively. Other constraints were minimum PDI and maximum entrapment efficiency. The composition of the optimized formulations is presented in Table 4. Formulation F 85 showed the highest residual value in terms of size (10.4 nm) and PDI (0.114), this value indicates how much the experimental value is far from the predicted value. The overall desirability value for these formulations (obtained using a desirability function that assigns numbers between 0 and 1 to the possible values each response with 0 representing a completely undesirable value and 1 representing the ideal response value) was 0.86 for F85 and was 0.78 for F 30. The good correlation between the actual and predicted results indicates that Box–Behnken design along with desirability function could be successfully used to optimize the nanoparticles manufacturing process.

Table 4. Composition of the optimized Ucuùba fat-based NLC formulations F 30 and F 85 along with the predicted, observed and residual values of the responses

Input Factors	**F 30**			**F 85**		
Surfactant (% w/v)	6			3		
Liquid Lipid (% w/v)	3			2.75		
Solid Lipid (% w/v)	7.63			7.68		
Responses	Predicted	Observed	Residual*	Predicted	Observed	Residual*
Size (nm)	30.0	33.6	-3.59	85.0	74.6	10.4
PDI	0.339	0.255	0.084	0.257	0.143	0.114
EE (%)	97.85	98.20	-0.35	97.67	98.70	-1.03

*Residual = Predicted – Observed

Figure **4** shows the TEM images of the NLC optimized formulations F30 and F85.

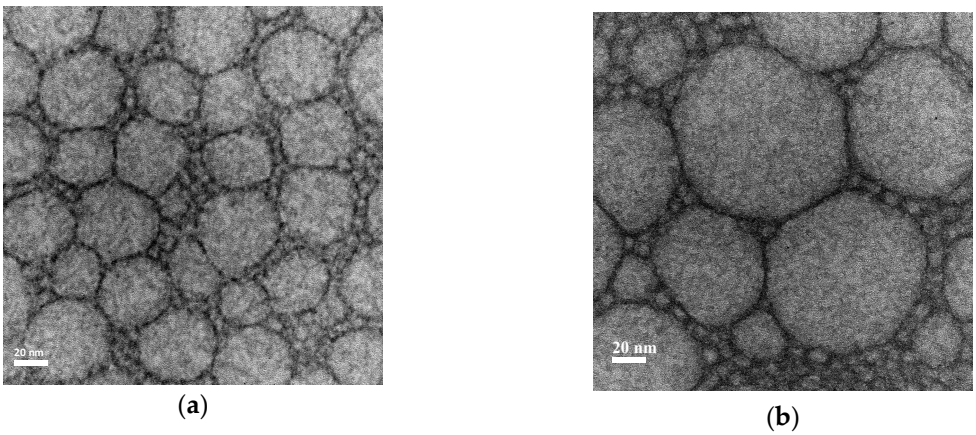

(**a**) (**b**)

Figure 4. Representative TEM images of the optimized Ucuùba fat-based NLC formulations **(a)** F 30 and **(b)** F 85.

The lipid nanoparticles displayed a globular shape, characterized by a spherical homogeneous lipid core surround by a surfactant corona. It can be appreciated from the images that particle size distribution appears quite uniform, as indicated by the low polydispersity index obtained with DLS measurements.

Peer-reviewed version available at Pharmaceutics 2019, 11, 284; doi:10.3390/pharmaceutics11060284

362 *3.2. Stability study of Ucuùba fat-based NLC prepared according to the optimized conditions*

363 Ucuùba fat-based NLC prepared according to the optimized conditions were characterized
364 immediately after preparation and up to 30 days of storage at room temperature. Results are shown
365 in **Table 5**.

366

367 **Table 5.** Physico- chemical characterization of optimized Ucuùba fat-based NLC during 30 days
368 storage at room temperature

Time (days)	F30			F85		
	Z- average (nm)	PDI	ζ potential (mV)	Z- average (nm)	PDI	ζ potential (mV)
0	33.6 ± 0.2	0.26 ± 0.01	-15.2 ± 0.8	74.6 ± 0.3	0.14 ± 0.00	-24.5 ± 0.6
1	33.7 ± 0.1	0.20 ± 0.01	-16.4 ± 1.3	74.1 ± 0.2	0.13 ± 0.02	-21.3 ± 1.1
7	34.4 ± 0.3	0.19 ± 0.00	-13.3 ± 1.1	72.9 ± 0.3	0.16 ± 0.04	-20.2 ± 6.5
15	33.3 ± 0.2	0.22 ± 0.01	-12.1 ± 1.3	71.1 ± 0.1	0.15 ± 0.01	-17.4 ± 0.6
30	33.8 ± 0.2	0.20 ± 0.01	-15.2 ± 0.8	73 ± 0.2	0.15 ± 0.01	-20.2 ± 1.5

369

370 The average particle size did not change significantly during the 30 days of observation.
371 Furthermore, the PDI of the optimized Ucuùba fat-based NLC were found to be below the values
372 0.16 and 0.26, respectively for F85 and F30, indicating a narrow particle size distribution and absence
373 of agglomerates for up to 30 days storage. All formulations exhibited negative zeta potential which
374 were around -15 mV and -25 mV, respectively for F30 and F85, and did not show significant changes
375 during the 30 days storage ($p>0.05$).

376

377 3.2.2 DSC

378 Differential Scanning Calorimetry is widely used for investigation the solid state of drugs and
379 excipients, such as lipids. In particular, thanks to the melting point identification and melting
380 enthalpies determination, this technique is interesting to highlight modifications of crystalline
381 components of the formulations, complementing the XRD data. The Ucuùba fat evidenced a melting
382 point of 43 °C (see Figure **5** and **Table 6**) while the blends of Ucuùba fat with Capryol 90 showed
383 lower melting points (see Figure **5a** and **Table 6**). At the same time a reduction of the melting enthalpy
384 was evident.

385

386

387

388

389

390

391

Peer-reviewed version available at Pharmaceutics 2019, 11, 284; doi:10.3390/pharmaceutics11060284

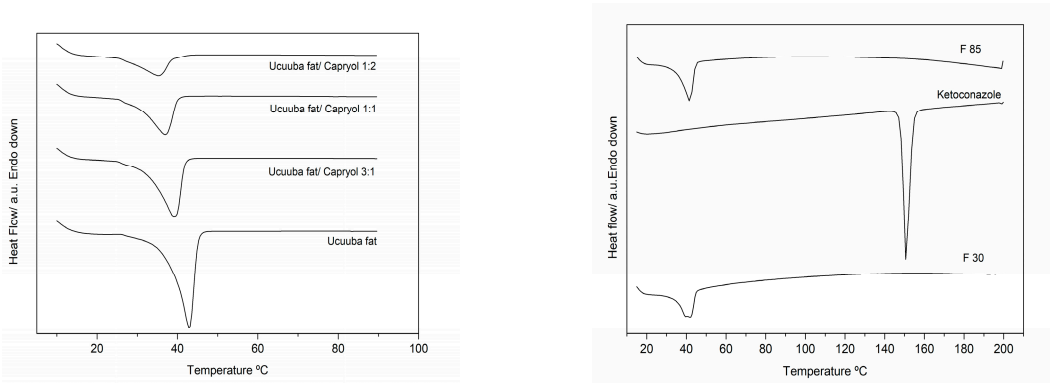

(**a**) (**b**)

Figure 5. DSC traces of Ucuùba fat/Capryol 90 mixtures (a) and of the optimized Ucuùba fat-based NLC formulations F 30 and F 85 along with ketoconazole raw material (b).

Table 6 shows the value CI which decreases with the increases of the amount Capriol 90. The data evidence that mixture with Capryol 90 influenced the order of Ucuùba fat crystalline lattice contributing to increase the lattice disorder causing the decrease crystalline index and a shift in the melting point to lower value. This last characteristic is desirable for the production of NCL, since a solid fat with less ordered lattice, reduces the probability of stability issues related to the expulsion of the entrapped active compound during storage [28].

Table 6. Melting temperatures, enthalpy and crystallinity index obtained by DSC analysis of the Ucuùba fat alone and in mixture with Capryol 90

Ucuùba fat / Capryol 90 weight ratio	T_{onset} (°C)	T_{endset} (°C)	Peak (°C)	Enthalpy (mJ)	CI (%)
1:0	37.76	45.11	42.99	562.72	100
3:1	31.96	41.77	39.79	493.38	65.75
1:1	28.90	40.00	36.98	452.26	40.18
1:2	26.61	38.91	35.24	260.32	15.16

The DSC results presented in Figure **5b** are related to ketoconazole and the two optimized formulations F30 and F85 after drying. It can be observed that only one endothermic peak appeared in the DSC traces obtained for both NLC formulations F30 and F85. For formulation F30 a single melting peak at 41.86°C and melting enthalpy of -89.13 J/g were observed during the heating process, attributed to lipid matrix solid-to-liquid transition. Similarly, also for F85 a single melting peak was evident at 41.59°C, corresponding to an enthalpy of -54.59 J/g were also related to the lipid matrix melting. Considering that ketoconazole showed an endothermic peak of fusion at 150.76°C, it can be inferred that ketoconazole is molecularly dispersed in the lipid matrix and no detectable drug crystals are formed during the production of the nanostructured lipid carriers.

3.2.3 XRD

Ucuùba fat is a mixture of mono-, di- and tri- triglycerides (trimyristin being the main component) characterized by a complex polymorphism that can be evidenced by X-ray diffraction. The diffractograms of the Ucuùba fat and the dried NLC formulations F 30 an F 85 are shown in Figure **6**. The diffraction pattern Ucuùba fat appears similar a diffraction pattern F 30 and F 85 (presence of

Peer-reviewed version available at Pharmaceutics 2019, 11, 284; doi:10.3390/pharmaceutics11060284

peaks at 2 theta 18.8°, 22.6° and 23. 5°), but the diffractograms of the NLC formulations show more broad and less defined peak indicating a solid state more amorphous than the virgin Ucuùba fat. This was expected also considering the presence in the NLC formulations of the liquid lipid Capryol 90, that as shown by DSC data, reduced the Amazonian fat organization.

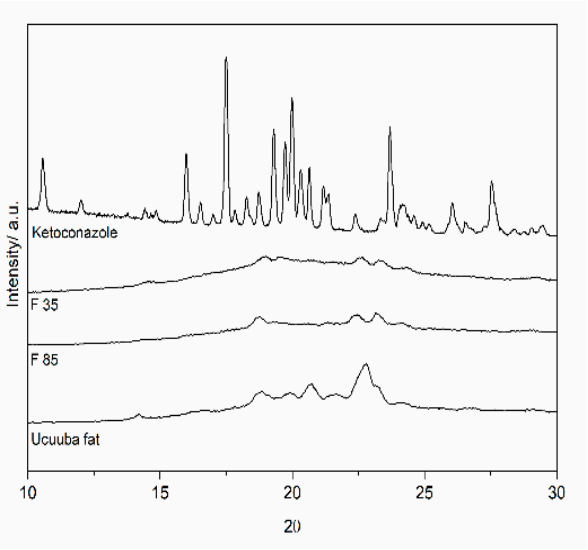

Figure 6. The X-ray diffraction spectra of Ucuùba fat and optimized Ucuùba fat-based NLC formulations F 30 and F 85.

At the same time it can be appreciated that of the numerous peaks characterizing the diffraction pattern of ketoconazole crystalline powder (see Figure **6**) none appears in the diffractogram obtained for ketoconazole-loaded NLC formulations F30 and F85, possibly indicating the ketoconazole is completely dispersed in the lipid matrix, even if due to the relatively low drug loading the presence of crystalline drug would be difficult to detect.

3.2.4 FTIR

Infrared spectroscopy (FTIR) is a valuable qualitative tool for characterization of the interaction of the components of pharmaceutical systems. FTIR analysis were performed for the main components of the nansostructured lipid carriers, *i.e.* Capryol 90, Ucuùba fat and ketoconazole, and the two Ucuùba fat-based NLC formulations (F 30 and F 85). The spectra are presented in Figure 7 and it appears clear that the FT-IR spectra of Ucuùba fat, Capryol 90 and NLC samples presented striking similarities and were almost superimposable. In these spectra, the high intensity peak at 1745 cm^{-1} corresponds to the vibration carbonyl groups [30]. The vibration of the C-O bond of ester bonds present in triacylglycerols is related to the sequence of peaks identified at 1232, 1165, 1118 and 1097 cm^{-1} [31]. The high intensity bands observed at 2922 and 2850 cm^{-1} are characteristic of the C-H stretching vibrations of lipids and correspond to olefinic (CH = CH) double bonds and methyl and methylene groups of fatty acid chains, respectively (Figure **7**) [32]. Overall these bands, that are characteristic of the lipid nature of Ucuùba fat and Capryol 90, are also strongly represented in the FTIR spectra of the NLC formulations in which the lipid matrix is the defining component.

Peer-reviewed version available at Pharmaceutics 2019, 11, 284; doi:10.3390/pharmaceutics11060284

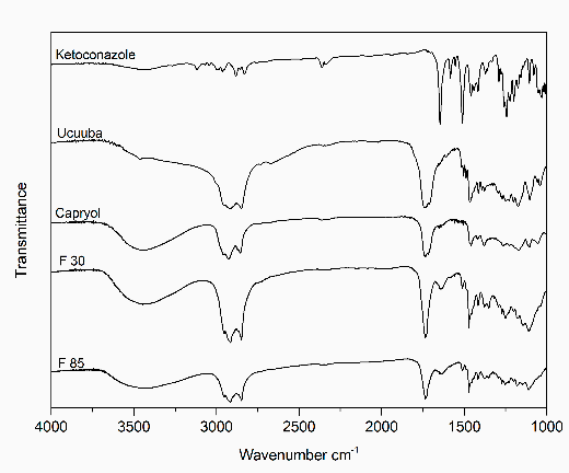

Figure 7. FT-IR spectra of ketoconazole, Ucuùba fat, Capryol 90 and of optimized Ucuùba fat-based NLC formulations F 30 and F 85.

The FT-IR spectrum of pure ketoconazole shows at least three characteristic peaks at 1647, 1510 and 1242 cm^{-1}, corresponding to the carbonyl (C=O), aromatic ring and C-N piperazine bonds stretching, respectively [33]. The spectrum ketoconazole in the spectra of formulations is almost completely disappeared, suggesting an efficient drug entrapment into the solid lipid nanoparticle matrix. However, the drug loading is demonstrated by the presence of weak bands between 1600 and 1650 and around 1250 cm^{-1}, not so evident in the FTIR spectra of lipid excipients.

4. Discussion

The main purpose of this study was the development and optimization Ucuùba fat- based NLC, using drug model the ketoconazole, for treatment onychomycosis. The pharmaceutical sector, since the introduction at starting of the new millennium of the Quality-by-Design approach, has started using systematically design of experiment as a statistical tool to maximize process knowledge and efficiently optimize product quality characteristics [34,35]. This approach has been applied to the manufacturing process of several dosage forms, including as tablets [36], pellets [37], semisolid formulations [38] and spray-dried powders to be used in dry powder inhalers [39].

However, DoE appears especially suitable for the development of innovative and complex dosage forms such as nanoparticles. In fact, scale-up manufacturing issues, lack of reproducibility with tight analytic standards and poor process control have been indicated as some of the critical underlying problems that hampered in the past the transfer of nanomedicines to the clinic [40]. At the same time, the potential of nanoformulations and in specific of lipid nanovectors for their inclusion for oral [41,42] or transmucosal drug products has not yet been fully tapped in[43–45].

For these reasons, in this study high-pressure homogenization, a robust and easy to scale up method, was selected for the manufacturing of nanostructured lipid carriers [46] and a Box-Behnken design (BBD) was applied to understand and optimize of Ucuùba fat-based NLC manufacturing process. The BBD allows to obtain a mathematical model describing as closely as possible effects of the factors and their levels on the critical quality attributes of the product, over the whole of the experimental domain, and also to predict the response inside domain [47].

The high-pressure homogenization manufacturing process led to a homogeneous, clear and transparent yellow-brownish dispersions, characteristic color of the Ucuùba fat. Particle size (Y_1) analysis confirmed that it was possible to obtain dispersions below 100 nm over all the experimental domain. Particle size was strongly influenced by TPGS and Ucuùba fat concentrations. The liquid lipid Capryol 90 influenced the particle size only in combination with TPGS (X_1X_2, p=0.0092) probably because it acts as co-surfactant in this formulation.

Peer-reviewed version available at Pharmaceutics 2019, 11, 284; doi:10.3390/pharmaceutics11060284

In particular, TPGS is a vitamin E derivative and a nonionic surfactant able to stabilize nanoemulsions by lowering interfacial tension with steric repulsion between nanoparticles. As a consequence, bigger amounts of surfactant result in smaller particle size [48]. Interestingly, TPGS has recently been shown to release by enzymatic cleavage of ester bonds tocopherol and tocopherol succinate [49]. Alpha-tocopherol has been demonstrated to be able to increase amphotericin B activity against *Candida albicans* [50]. Therefore, the surfactant increase could not only contribute to particle size decrease, but high TPGS concentrations could result in an enhanced antifungal activity of ketoconazole.

PDI (Y_2) values ranged from 0.248 to 0.558. This parameter reflects homogeneity of nanoparticle populations, values lower than 0.3 indicating relatively narrow particle size distribution and values even lower associated with monodisperse particles are generally desirable. Higher values are on the contrary associated to polydisperse particle size distribution [51]. In our DoE, formulations with high surfactant concentration showed PDI values above 0.4 and multimodal size distribution. The correlation among surfactant concentration and increasing PDI value could explained considering that an excess of TPGS tends to self-assemble into micelles. Furthermore, it is possible that during the Ucuùba fat-based NLC preparation with high pressure homogenizer the temperature increase could have decreased the TPGS critical micelle concentration (CMC) and favoured the production of different micelle populations leading to PDI increase [29].

Concerning ketoconazole encapsulation efficiency was found to range from 93.91 to 99.66 %. The encapsulation efficiency in this work was found not to depend in a statistically significant manner from the process parameters explored. Probably this result was obtained because the percentage ketoconazole was maintained constant in all formulations (0.5% w/v ketoconazole) and Ucuùba fat-based NLC offered sufficient lipid matrix to fully solubilize and encapsulate ketoconazole inside nanoparticles. The lipid phase NLC is the mixture of the solid and liquid lipids, in this work Ucuùba fat was the choice for the solid lipid and Capryol is the liquid lipid. This peculiarity of NLC is the reason for its higher encapsulation efficiency and better storage stability when compared to solid lipid nanoparticles (SLN) [52]. In particular, the DSC thermograms of Ucuùba fat was found to be affected by the mixing with Capryol and it was observed that increasing the ratio of Capryol a broadening of the meting peak of the solid fat was observed, possibly indicating the formation of several polymorphic forms. Similarly,[53] studied the effect of the addition of α-tocopherol on the crystalline organization of Compritol® ATO 888, for NLC production, and observed that the addition of 30% α-tocopherol decreases the melting point of Compritol from 71° C to 50.3° C. The authors explained this melting point decrease to the appearance of less organized polymorphic arrangements in the solid lipid due to the addition of α-tocopherol.

In order to study lipid matrix crystalline organization, X-ray diffraction is a widely used technique also for the investigation of SLN and NLC [54]. The lipid polymorphism is a property that allows the triglycerides to exist in the form of several crystalline structures in different molecular packages[55]. The three most common types of packaging of triglycerides are hexagonal, orthorhombic and triclinic, which are usually referred to as polymorphic forms α, β 'and β, respectively. The type of crystalline form depends on the molecular structure and composition of the lipids, as well as the environmental conditions during storage (cooling rate, for example). For the Ucuùba fat based- NLC, the sharp peaks at were at 18.9°, 22.6° and 23.2°, which correspond to short spacings at 0.46 nm, 0.393 nm and 0.382 nm indicative of β e β', respectively [55,56]. The measurements of crystallinity and lipid modification are strongly connected with drug release and drug incorporation [55].

Zeta potential values are often used to predict the stability of nanoparticles. In fact, this parameter reflects the charge of the surface of nanoparticles in suspensions and high zeta potential values indicate high repulsive forces between particles, preventing them from forming large particle size agglomerates [10,51,57,58]. In general, nanomaterials with zeta potential above 30 mV are considered highly stable [59,60]. However, in our DoE the zeta potential absolute values were found to be smaller than 30 mV. However, these systems which contain a steric stabilizer, such as the non-ionic and PEGylated TPGS and as a consequence, the absorption of the steric stabilizer on nanoparticle surface decreases the zeta potential due the shift of the shear plane of the electrical double layer existing

Peer-reviewed version available at Pharmaceutics 2019, 11, 284; doi:10.3390/pharmaceutics11060284

around each particles [10] but it provides a steric contribution to particle stability due the presence of the hydrophilic polymer chains [43].

5. Conclusions

In this study, nanostructured lipid carriers formulated using an Amazonian fat were manufactured using a high-pressure homogenizer and the process was studied and optimized using a design of experiment approach. Results obtained allowed to build a predictive mathematical model showing that among the critical process parameters studied surfactant and Ucuùba fat concentrations were the most significant factors for the determination of the nanoparticles average size and particle size distribution in terms of polydispersity index. The encapsulation efficiency was found to be above 90% for all the experimental design space and factors selected did not significantly affect its value in this model.

Using the model obtained with the design of experiment, two optimized NLC formulations, one with low (30 nm) and high particle size (85 nm) and both characterized by low PDI and high encapsulation efficiency. The optimized nanoparticles were successfully obtained and were stable during the 30 days, in which there was no significant change in the values of PDI, zeta potential and particle size. The analysis of the XDR and DSC analysis were excellent tools for the characterization of the crystal order the formulation, showed that formulations the decrease the crystal order formulations when compared Ucuùba fat. The total absence of the ketoconazole signals in the DSC thermograms and XDR spectra, suggested an optimal drug encapsulation and no sign of drug expulsion.

The optimized formulations obtained will be further investigated for their topical application against onychomycosis.

Author Contributions: Conceptualization, J.O.C.S.J., R.M.R.C., and F.S.; methodology, R.R.P., M.T., F.R.; investigation, R.R.P.; M.T.; writing—original draft preparation, R.R.P..; writing—review and editing, R.R.P., F.S. and R.B.; supervision, C.P., F.S..; funding acquisition, R.B., P.S. and J.O.C.S.J.

Funding: This study was supported by CAPES (Coordenação de Aperfeiçoamento de Pessoal de Nível Superior – Brazil).

Conflicts of Interest: The authors declare no conflict of interest.

Peer-reviewed version available at Pharmaceutics 2019, 11, 284; doi:10.3390/pharmaceutics11060284

References

1. Murdan, S. Drug delivery to the nail following topical application. *International Journal of Pharmaceutics* **2002**, *236*, 1–26, doi:10.1016/S0378-5173(01)00989-9.

2. McAuley, W. J.; Jones, S. A.; Traynor, M. J.; Guesné, S.; Murdan, S.; Brown, M. B. An investigation of how fungal infection influences drug penetration through onychomycosis patient's nail plates. *European Journal of Pharmaceutics and Biopharmaceutics* **2016**, *102*, 178–184, doi:10.1016/j.ejpb.2016.03.008.

3. Laffleur, F.; Ataii, M. Preparation and evaluation of a novel dosage form for onychomycosis. *International Journal of Pharmaceutics* **2017**, *518*, 105–110, doi:10.1016/j.ijpharm.2016.12.055.

4. Mahtab, A.; Anwar, M.; Mallick, N.; Naz, Z.; Jain, G. K.; Ahmad, F. J. Transungual Delivery of Ketoconazole Nanoemulgel for the Effective Management of Onychomycosis. *AAPS PharmSciTech.* **2016**, doi:10.1208/s12249-016-0488-0.

5. Gunt, H. B.; Kasting, G. B. Effect of hydration on the permeation of ketoconazole through human nail plate in vitro. *European Journal of Pharmaceutical Sciences* **2007**, *32*, 254–260, doi:10.1016/j.ejps.2007.07.009.

6. Lin, C.; Wedeen, V. J.; Chen, J.; Yao, C.; Tseng, W. I. Article in press. *Design* **2003**, *0*, 1–5, doi:10.1016/S1053-8119(03)00154-X.

7. Bseiso, E. A.; Nasr, M.; Sammour, O. A.; Abd El Gawad, N. A. Novel nail penetration enhancer containing vesicles "nPEVs" for treatment of onychomycosis. *Drug Delivery* **2016**, *23*, 2813–2819, doi:10.3109/10717544.2015.1099059.

8. Kumar, S.; Randhawa, J. K. High melting lipid based approach for drug delivery: solid lipid nanoparticles. *Materials science & engineering Materials for biological applications.* **2013**, *33*, 1842–52, doi:10.1016/j.msec.2013.01.037.

9. Müller, R. H.; Radtke, M.; Wissing, S. A. Solid lipid nanoparticles (SLN) and nanostructured lipid carriers (NLC) in cosmetic and dermatological preparations. *Advanced Drug Delivery Reviews* **2002**, *54*, 131–155, doi:10.1016/S0169-409X(02)00118-7.

10. Müller, R. H.; Mäder, K.; Gohla, S. Solid lipid nanoparticles (SLN) for controlled drug delivery â " a review of the state of the art. *European Journal of Pharmaceutics and Biopharmaceutics* **2000**, *50*, 161–177, doi:10.1016/S0939-6411(00)00087-4.

11. Jenning, V.; Gysler, A.; Schafer-Korting, M.; Gohla, S. H. Vitamin A loaded solid lipid nanopartcles for topical use: occlusive properties and drug trageting to the upper skin. *Eur. J. Pharm. Biopharm.* **2000**, *49*, 211–218.

12. Garcês, A.; Amaral, M. H.; Sousa Lobo, J. M.; Silva, A. C. Formulations based on solid lipid nanoparticles (SLN) and nanostructured lipid carriers (NLC) for cutaneous use: A review. *European Journal of Pharmaceutical Sciences* **2017**, *112*, 159–167, doi:10.1016/j.ejps.2017.11.023.

13. Rocha, K. A. D.; Krawczyk-Santos, A. P.; Andrade, L. M.; Souza, L. C. de; Marreto, R. N.; Gratieri, T.; Taveira, S. F. Voriconazole-loaded nanostructured lipid carriers (NLC) for drug delivery in deeper regions of the nail plate. *International Journal of Pharmaceutics* **2017**, *531*, 292–298, doi:10.1016/j.ijpharm.2017.08.115.

14. Venturini, C. G.; Bruinsmann, F. A.; Contri, R. V.; Fonseca, F. N.; Frank, L. A.; D'Amore, C. M.; Raffin, R. P.; Buffon, A.; Pohlmann, A. R.; Guterres, S. S. Co-encapsulation of imiquimod and copaiba oil in novel nanostructured systems: Promising formulations against skin carcinoma. *European Journal of Pharmaceutical Sciences* **2015**, *79*, 36–43, doi:10.1016/j.ejps.2015.08.016.

15. Pinto, F.; de Barros, D. P. C.; Fonseca, L. P. Design of multifunctional nanostructured lipid carriers enriched with α-tocopherol using vegetable oils. *Industrial Crops and Products* **2018**, *118*, 149–159, doi:10.1016/j.indcrop.2018.03.042.

16. Pardauil, J. J. R.; de Molfetta, F. A.; Braga, M.; de Souza, L. K. C.; Filho, G. N. R.; Zamian, J. R.; da Costa, C. E. F. Characterization, thermal properties and phase transitions of amazonian vegetable oils. *Journal of Thermal Analysis and Calorimetry* **2016**, 1–9, doi:10.1007/s10973-016-5605-5.

17. Lourith, N.; Kanlayavattanakul, M.; Mongkonpaibool, K.; Butsaratrakool, T.; Chinmuang, T. Rambutan seed as a new promising unconventional source of specialty fat for cosmetics. *Industrial Crops and Products* **2016**, *83*, 149–154, doi:10.1016/j.indcrop.2015.12.045.

18. Stecanella, L. A.; Taveira, S. F.; Marreto, R. N.; Valadares, M. C.; Vieira, M. de S.; Kato, M. J.; Lima, E. M. Development and characterization of PLGA nanocapsules of grandisin isolated from Virola surinamensis: In vitro release and cytotoxicity studies. *Brazilian Journal of Pharmacognosy* **2013**, *23*, 153–159, doi:10.1590/S0102-695X2012005000128.

19. Serra, J. L.; Silva, L. H. M. da; Meirelles, A. J. de A.; Darnet, S. H.; de Freitas, R. A.; Rodrigues, A. M. da C. Alternative sources of oils and fats from Amazonian plants: Fatty acids, methyl tocols, total carotenoids and chemical composition. *Food Research International* **2018**, *116*, 12–19, doi:10.1016/j.foodres.2018.12.028.

20. Lopes, N. P.; Kato, M. J.; Yoshida, M. Antifungal constituents from roots of Virola surinamensis. *Phytochemistry* **1999**, *51*, 29–33, doi:10.1016/S0031-9422(98)00709-2.

21. Pagnocca, F. C.; Ribeiro, S. B.; Torkomian, V. L. V.; Hebling, M. J. A.; Bueno, O. C.; Da Silva, O. A.; Fernandes, J. B.; Vieira, P. C.; Da Silva, M. F. D. G. F.; Ferreira, A. G. Toxicity of lignans to symbiotic fungus of leaf-cutting ants. *Journal of Chemical Ecology* **1996**, *22*, 1325–1330, doi:10.1007/BF02266969.

22. Zacchino, S.; Rodríguez, G.; Pezzenati, G.; Orellana, G.; Enriz, R.; Sierra, M. G. In vitro evaluation of antifungal properties of 8.O.4'-Neolignans. *Journal of Natural Products* **1997**, *60*, 659–662, doi:10.1021/np9605504.

23. Hao, J.; Fang, X.; Zhou, Y.; Wang, J.; Guo, F.; Li, F.; Peng, X. Development and optimization of solid lipid nanoparticle formulation for ophthalmic delivery of chloramphenicol using a Box-Behnken design. *International Journal of Nanomedicine* **2011**, *6*, 683–692, doi:10.2147/IJN.S17386.

Peer-reviewed version available at Pharmaceutics 2019, 11, 284; doi:10.3390/pharmaceutics11060284

24. Baig, M. S.; Ahad, A.; Aslam, M.; Imam, S. S.; Aqil, M.; Ali, A. Application of Box-Behnken design for preparation of levofloxacin-loaded stearic acid solid lipid nanoparticles for ocular delivery: Optimization, in vitro release, ocular tolerance, and antibacterial activity. *International Journal of Biological Macromolecules* **2016**, *85*, 258–270, doi:10.1016/j.ijbiomac.2015.12.077.

25. Badawi, N. M.; Hteaima, M. H.; El-Say, K. M.; Aattia, D. A.; Ael-Nabarawi, M. A.; Elmazar, M. M. Pomegranate extract-loaded solid lipid nanoparticles: Design, optimization, and in vitro cytotoxicity study. *International Journal of Nanomedicine* **2018**, *13*, 1313–1326, doi:10.2147/IJN.S154033.

26. Wani, T. A.; Ahmad, A.; Zargar, S.; Khalil, N. Y.; Darwish, I. A. Use of response surface methodology for development of new microwell-based spectrophotometric method for determination of atrovastatin calcium in tablets. *Chemistry Central Journal* **2012**, 6:134, 1–9, doi: 10.1186/1752-153X-6-134.

27. Asghar, A.; Abdul Raman, A. A.; Daud, W. M. A. W. A comparison of central composite design and Taguchi method for optimizing Fenton process. *The Scientific World Journal* **2014**, doi:10.1155/2014/869120.

28. Pradhan, M.; Singh, D.; Singh, M. R. Fabrication, optimization and characterization of Triamcinolone acetonide loaded nanostructured lipid carriers for topical treatment of psoriasis: Application of Box Behnken design, in vitro and ex vivo studies. *Journal of Drug Delivery Science and Technology* **2017**, *41*, 325–333, doi:10.1016/j.jddst.2017.07.024.

29. Severino, P.; Santana, M. H. A.; Souto, E. B. Optimizing SLN and NLC by 2 2 full factorial design: Effect of homogenization technique. *Materials Science and Engineering C* **2012**, *32*, 1375–1379, doi:10.1016/j.msec.2012.04.017.

30. Dos Santos Costa, M. N. F.; Muniz, M. A. P.; Negrão, C. A. B.; Da Costa, C. E. F.; Lamarão, M. L. N.; Morais, L.; Silva Júnior, J. O. C.; Ribeiro Costa, R. M. Characterization of Pentaclethra macroloba oil: Thermal stability, gas chromatography and Rancimat. *Journal of Thermal Analysis and Calorimetry* **2014**, *115*, 2269–2275, doi:10.1007/s10973-012-2896-z.

31. Del Rio, J. C.; Evaristo, A. B.; Marques, G.; Martín-Ramos, P.; Martín-Gil, J.; Gutiérrez, A. Chemical composition and thermal behavior of the pulp and kernel oils from macauba palm (Acrocomia aculeata) fruit. *Industrial Crops and Products* **2016**, *84*, 294–304, doi:10.1016/j.indcrop.2016.02.018.

32. Shapaval, V.; Afseth, N. K.; Vogt, G.; Kohler, A. Fourier transform infrared spectroscopy for the prediction of fatty acid profiles in Mucor fungi grown in media with different carbon sources. *Microbial Cell Factories* **2014**, *13*, 1–11, doi:10.1186/1475-2859-13-86.

33. Karolewicz, B.; Górniak, A.; Owczarek, A.; Zurawska-Płaksej, E.; Piwowar, A.; Pluta, J. Thermal, spectroscopic, and dissolution studies of ketoconazole-Pluronic F127 system. *Journal of Thermal Analysis and Calorimetry* **2014**, *115*, 2487–2493, doi:10.1007/s10973-014-3661-2.

34. Csóka I, Pallagi E, Paál TL. Extension of quality-by-design concept to the early development phase of pharmaceutical R&D processes. *Drug Discov Today* **2018**, 23(7):1340-1343. doi: 10.1016/j.drudis.2018.03.012

Peer-reviewed version available at *Pharmaceutics* **2019**, *11*, 284; doi:10.3390/pharmaceutics11060284

35. Politis, S. N.; Colombo, P.; Colombo, G.; Rekkas, D. M. Design of experiments (DoE) in pharmaceutical development. *Drug Development and Industrial Pharmacy* **2017**, *43*, 889–901, doi:10.1080/03639045.2017.1291672.

36. Oh, G. H.; Park, J. H.; Shin, H. W.; Kim, J. E.; Park, Y. J. Quality-by-design approach for the development of telmisartan potassium tablets. *Drug Development and Industrial Pharmacy* **2018**, *44*, 837–848, doi:10.1080/03639045.2017.1414233.

37. Politis, S. N.; Rekkas, D. M. Development of a fast, lean and agile direct pelletization process using experimental design techniques. *Drug Development and Industrial Pharmacy* **2017**, *43*, 545–557, doi:10.1080/03639045.2016.1269121.

38. Bakonyi, M.; Berkó, S.; Kovács, A.; Budai-Szűcs, M.; Kis, N.; Erős, G.; Csóka, I.; Csányi, E. Application of quality by design principles in the development and evaluation of semisolid drug carrier systems for the transdermal delivery of lidocaine. *Journal of Drug Delivery Science and Technology* **2018**, *44*, 136–145, doi:10.1016/j.jddst.2017.12.001.

39. Belotti, S.; Rossi, A.; Colombo, P.; Bettini, R.; Rekkas, D.; Politis, S.; Colombo, G.; Balducci, A. G.; Buttini, F. Spray dried amikacin powder for inhalation in cystic fibrosis patients: A quality by design approach for product construction. *International Journal of Pharmaceutics* **2014**, *471*, 507–515, doi:10.1016/j.ijpharm.2014.05.055.

40. Eaton, M. A. W.; Levy, L.; Fontaine, O. M. A. Delivering nanomedicines to patients: A practical guide. *Nanomedicine: Nanotechnology, Biology, and Medicine* **2015**, *11*, 983–992, doi:10.1016/j.nano.2015.02.004.

41. Garrastazu Pereira, G.; Rawling, T.; Pozzoli, M.; Pazderka, C.; Chen, Y.; Dunstan, C.; Murray, M.; Sonvico, F. Nanoemulsion-Enabled Oral Delivery of Novel Anticancer ω-3 Fatty Acid Derivatives. *Nanomaterials* **2018**, *8*, 825, doi:10.3390/nano8100825.

42. Uner M, Damgalı S, Ozdemir S, Celik B. Therapeutic potential of drug delivery by means of lipid nanoparticles: reality or illusion? *Current Pharmaceutical Desing* **2017**; 23(43):6573-6591, doi: 10.2174/1381612823666171122110638

43. Rossi, I.; Sonvico, F.; McConville, J. T.; Rossi, F.; Fröhlich, E.; Zellnitz, S.; Rossi, A.; Del Favero, E.; Bettini, R.; Buttini, F. Nebulized coenzyme Q10 nanosuspensions: A versatile approach for pulmonary antioxidant therapy. *European Journal of Pharmaceutical Sciences* **2018**, *113*, 159–170, doi:10.1016/j.ejps.2017.10.024.

44. Sánchez-lópez, E.; Espina, M.; Doktorovova, S.; Souto, E. B.; García, M. L. Lipid nanoparticles (SLN , NLC): Overcoming the anatomical and physiological barriers of the eye – Part II - Ocular drug-loaded lipid nanoparticles. *European Journal of Pharmaceutics and Biopharmaceutics* **2017**, *110*, 58–69, doi:10.1016/j.ejpb.2016.10.013.

45. Comfort C., Garrastazu G., Pozzoli M., Sonvico F. Opportunities and Challenges for the Nasal Administration of Nanoemulsions. *Current Topics Medicinal Chemistry*, **2015**, *15* (4), 356-368.

46. Müller, R. H.; Shegokar, R.; Keck, C. M. 20 Years of Lipid Nanoparticles (SLN & NLC): Present State of Development & Industrial Applications. *Current Drug Discovery Technologies* **2011**, *8*, 207–227.

47. Agyralides, G. G.; Dallas, P. P.; Rekkas, D. M. Development and in vitro evaluation of furosemide transdermal formulations using experimental design techniques. *International Journal of Pharmaceutics* **2004**, *281*, 35–43, doi:10.1016/j.ijpharm.2004.05.011.

48. Mehmood, T.; Ahmad, A.; Ahmed, A.; Ahmed, Z. Optimization of olive oil based O / W nanoemulsions prepared through ultrasonic homogenization : A response surface methodology approach. *Food Chemistry* **2017**, *229*, 790–796, doi:10.1016/j.foodchem.2017.03.023.

49. Grimaudo, M. A.; Pescina, S.; Padula, C.; Santi, P.; Concheiro, A.; Alvarez-Lorenzo, C.; Nicoli, S. Poloxamer 407/TPGS Mixed Micelles as Promising Carriers for Cyclosporine Ocular Delivery. *Molecular Pharmaceutics* **2018**, *15*, 571–584, doi:10.1021/acs.molpharmaceut.7b00939.

50. Belhachemi, M. H.; Boucherit, K.; Boucherit-Otmani, Z.; Belmir, S.; Benbekhti, Z. Original article/Article original: Effects of ascorbic acid and α-tocopherol on the therapeutic index of amphotericin B. *Effet de l'acide ascorbique et de α-tocophérol sur l'index thérapeutique de l'amphotéricine B (French)*. *Journal de Mycologie Médicale* **2014**, 6–11, doi.org/10.1016/j.mycmed.2014.04.003

51. Mun, A.; Ping, C.; Lin, K. Physicochemical , oxidative and anti-oxidant stabilities of kenaf seed oil-in-water nanoemulsions under different storage temperatures. *Industrial Crops & Products* **2017**, *95*, 374–382, doi:10.1016/j.indcrop.2016.10.047.

52. Tamjidi, F.; Shahedi, M.; Varshosaz, J.; Nasirpour, A. Nanostructured lipid carriers (NLC): A potential delivery system for bioactive food molecules. *Innovative Food Science and Emerging Technologies* **2013**, *19*, 29–43, doi:10.1016/j.ifset.2013.03.002.

53. Souto, E. B.; Mehnert, W.; Müller, R. H. Polymorphic behaviour of Compritol??888 ATO as bulk lipid and as SLN and NLC. *Journal of Microencapsulation* **2006**, *23*, 417–433, doi:10.1080/02652040600612439.

54. Bunjes, H.; Unruh, T. Characterization of lipid nanoparticles by differential scanning calorimetry, X-ray and neutron scattering. *Advanced Drug Delivery Reviews* **2007**, *59*, 379–402, doi:10.1016/j.addr.2007.04.013.

55. De Carvalho, S. M.; Noronha, C. M.; Floriani, C. L.; Lino, R. C.; Rocha, G.; Bellettini, I. C.; Ogliari, P. J.; Barreto, P. L. M. Optimization of α-tocopherol loaded solid lipid nanoparticles by central composite design. *Industrial Crops and Products* **2013**, *49*, 278–285, doi:10.1016/j.indcrop.2013.04.054.

56. Bouzidi, L.; Narine, S. S. Relationships between molecular structure and kinetic and thermodynamic controls in lipid systems. Part II: Phase behavior and transformation paths of SSS, PSS and PPS saturated triacylglycerols - Effect of chain length mismatch. *Chemistry and Physics of Lipids* **2012**, *165*, 77–88, doi:10.1016/j.chemphyslip.2011.11.005.

57. Butt, U.; ElShaer, A.; Snyder, L.; Al-Kinani, A.; Le Gresley, A.; Alany, R. Fatty Acid Based Microemulsions to Combat Ophthalmia Neonatorum Caused by Neisseria gonorrhoeae and Staphylococcus aureus. *Nanomaterials* **2018**, *8*, 51, doi:10.3390/nano8010051.

Peer-reviewed version available at *Pharmaceutics* **2019**, *11*, 284; doi:10.3390/pharmaceutics11060284

742 58. Toropov, A. A.; Sizochenko, N.; Toropova, A. P.; Leszczynski, J. Towards the development of global
743 nano-quantitative structure–property relationship models: Zeta potentials of metal oxide nanoparticles.
744 *Nanomaterials* **2018**, *8*, doi:10.3390/nano8040243.

745 59. Bitencourt, A. P. R.; Duarte, J. L.; Oliveira, A. E. M. F. M.; Cruz, R. A. S.; Carvalho, J. C. T.; Gomes, A. T.
746 A.; Ferreira, I. M.; Ribeiro-Costa, R. M.; Silva-Júnior, J. O. C.; Fernandes, C. P. Preparation of aqueous
747 nanodispersions with annatto (Bixa orellana L.) extract using an organic solvent-free and low energy
748 method. *Food Chemistry* **2018**, *257*, 196–205, doi:10.1016/j.foodchem.2018.02.067.

749 60. Bhattacharjee, S. Review article DLS and zeta potential – What they are and what they are not ? *Journal*
750 *of Controlled Release* **2016**, *235*, 337–351, doi:10.1016/j.jconrel.2016.06.017.